

Sedimentation potential of a concentrated spherical colloidal suspension

計劃編號: NSC89-2214-E-002-003

執行期限: 88/08/01-89/07/31

主持人: 李克強 台灣大學化工系 教授

一、中文摘要(關鍵詞: 電泳, 電位, 電雙層極化, 懸浮溶液)

本研究為了解帶電密集膠體溶液之沈降理論, 在本研究中考慮了電雙層極化效應, 使用細胞模式來描述多顆粒子之系統, 使用假光譜法來求解主控電動方程式, 其中有流場之 Navier-Stokes 方程式, 電場之 Poisson 方程式, 發現了一些有趣的現象, 如沈降電位在表面電位小時有最小值, 而在表面電位大時有最大值。

ABSTRACT(Key words: sedimentation, potential, double layer polarization, suspension)

The sedimentation behavior of a concentrated suspension of charged spherical particles is investigated theoretically. The sedimentation potential is evaluated taking the effect of double layer polarization into account. A cell model is adopted to describe the present multi-entities system, and a pseudo-spectral numerical scheme is used to solve the governing electrokinetic equations, which comprise a Navier-Stokes equation for flow field and a Poisson equation for electric field. Several interesting phenomena, which are absent if double layer polarization is neglected, are observed. For example, the ratio (E^*/U^*) , E^* and U^* being respectively the scaled sedimentation potential has a minimum if the electrical potential is low, and has a maximum if it is high.

二、計劃緣由與目的

Gravitational sedimentation of charged particles is one of the basic electrokinetic phenomena of colloidal suspensions. It is similar to the electrophoresis of charged particles, and sedimentation potential is found to correlate with electrophoretic mobility, the so-called Onsager relation.^{1,2} If the concentration of particles is appreciable, the interaction between adjacent particles may play a significant role, and the problem becomes complicated. Levine and Neale³ discussed the electrophoresis of concentrated spherical particles at low electrical potential by adopting the cell model proposed by Kuwabara.⁴ This model assumes that the system under consideration can be simulated by a swarm of cells, each comprises a particle and a concentric spherical shell of liquid phase. Assuming low surface potential and thin electrical double layer, i.e., the interaction between adjacent double layers is negligible, Levine et al.⁵ were able to derive an analytical expression for both the sedimentation potential and the velocity of particles of a concentrated colloidal suspension. Under the same condition, Ohshima⁶ derived the electrophoretic mobility of a concentrated colloidal suspension. The cell model was also used to derive the electrophoretic mobility

of a concentrated spherical dispersion under the condition of thin electrical double layers.^{7,8} A more general analysis, which is based on an arbitrary level of surface potential and thickness of double layer, was presented recently by Lee, et al.⁹

Compared with the electrophoresis, relative attention has been paid to the sedimentation behavior of a colloidal suspension, presumably due to the fact that the effect of double layer relaxation involved cannot be neglected at the first place as in electrophoresis. The result of Levine et al.⁵ for sedimentation potential are consistent with limited experimental data, and thus provided an indirect evidence for the applicability of cell model. However, in order to obtain an analytical expression, they made several simplifications that reduced the generality considerably. First, using the linearized version of the Poisson-Boltzmann equation which describes the spatial variation of electrical potential is suited for a surface potential lower than 25 mV. Second, the terms involving the electric effects in the hydrodynamic equation are neglected. Third, the double layer interaction between adjacent cells is neglected, which is reasonable if $ka \gg 1$, a and $1/\kappa$ being respectively the particle radius and double layer thickness. Levine and Neale³ pointed out that it is necessary to develop a more general model for the case of higher potentials and smaller values of ka in which the effect of double layer polarization becomes much more significant. In a recent study, Ohshima¹⁰ was able to derive an Onsager relation between electrophoresis and sedimentation under the same condition of Levine et al.⁵

In the present study, the analyses of Levine et al.⁵ and Ohshima¹⁰ are extended to the case that the surface potential is not necessarily low and the effect of double layer polarization may be significant.

三、研究方法和成果

We consider identical, non-conducting, spherical particles of radius a in a $z_1:z_2$ electrolyte solution, z_1 and z_2 being respectively the valences of cations and anions. If we let $\alpha = -z_1/z_2$, then the electroneutrality in the bulk liquid phase requires that $n_{z_2} = n_{z_1}/\alpha$. Referring to Fig.1, the cell model of Kuwabara⁴ is used where each particle is surrounded by a concentric spherical shell of liquid phase of radius b . The spherical coordinates, (r, θ, ϕ) , with its origin located at the center of the particle are adopted in the following analysis. Due to an electric field E is induced in the z -direction ($\theta=0$). Suppose that the liquid phase is incompressible and has constant physical properties. Also, the motion of particles is slow so that the system under consideration is at a quasi-steady state. Then, the

conservation of ions leads to

$$\bar{\nabla} \bullet \left[D_j \left[\bar{\nabla} n_j + \frac{z_j e n_j}{kT} \bar{\nabla} \phi \right] + n_j \bar{v} \right] = 0, j=1,2$$

where $\bar{\nabla}$ denotes the gradient operator, e and ϕ are respectively the elementary charge and the electrical potential, \bar{v} represents the fluid velocity, k and T are the Boltzmann constant and the absolute temperature respectively, and n_j , D_j , and z_j are the number concentration, the diffusivity, and the valence of ion species j respectively.

If the time scale for double-layer relaxation is much smaller than that of the motion of a particle, then the spatial variation of the electrical potential can be described by the Poisson-Boltzmann equation

$$\nabla^2 \phi = - \sum_{j=1}^2 \frac{z_j e n_j}{\epsilon}$$

where ϵ denotes the permittivity of the liquid phase.

The flow field is described by the Navier-Stokes equation in the creeping flow region

$$\bar{\nabla} \bullet \bar{v} = 0$$

$$\eta \nabla^2 \bar{v} - \bar{\nabla} p - \rho \bar{\nabla} \phi = 0$$

In these expressions p , η , and ρ denote respectively the pressure, the viscosity, and the density of fluid.

Suppose that ϕ can be decomposed as $\phi = \phi_1 + \phi_2$ where ϕ_1 and ϕ_2 represent respectively the electrical potential that would exist in the absence of the induced electric field, and that outside a particle arising from the induced electric field. Then the effect of double-layer polarization is taken into account by considering the expression¹²

$$n_j = n_{j0} \exp \left(- \frac{z_j e (\phi_1 + \phi_2 + g_j)}{kT} \right), j=1,2$$

where g_j denotes a function which accounts the effects of fluid flow on concentration, i.e., the effect of double-layer polarization. If ϕ_2 and g_j are small, Eq.(6) can be linearized as

$$n_j = \exp \left(- \frac{z_j e \zeta_a}{kT} \phi_1^* \right) \left[1 - \frac{z_j e \zeta_a}{kT} (\phi_2^* + g_j^*) \right], j=1,2$$

where, $\phi^* = \phi / \zeta_a$, $g_j^* = g_j / \zeta_a$ and the surface potential of a particle is characterized by, ζ_a zeta potential at the particle surface.

The ratio E^* / U^* , which is a measure for the induced sedimentation potential per unit sedimentation velocity, can be evaluated based on the fact that the sedimentation of particles generates no net current, or the net flow of current across any horizontal plane vanishes, the condition of streaming potential. We apply this condition to the horizontal plane, $\theta = \pi/2$. If we define the net current as $\langle i \rangle$, then

$$\langle i \rangle = 0 = 2\pi \int_a^b r i_\theta dr \Big|_{\theta = \frac{\pi}{2}}$$

$$= 2\pi \int_a^b r \left(\sum z_j e n_j v_{j\theta} \right) dr \Big|_{\theta = \frac{\pi}{2}}, j = 1, 2$$

where i_θ is the θ -component of current i .

$$i = \sum z_j e n_j \bar{v}_j$$

and v_{θ} is the θ -component of the flow velocity of the j th ionic species, v_j . The θ -component of i is used since it is the normal component of the current density to the plane $\theta = \pi/2$, and v_j , the flow velocity of the whole electrolyte solution. According to O'Brien and White,¹² the problem of solving (8)-(13f) can be decomposed into two sub-problems: (a) a particle moves at a uniform velocity U in the absence of the induced electric field, and (b) the particle is held fixed in the induced electric field. These problems are denoted as problems 1 and 2 hereafter. The net current across the plane $\theta = \pi/2$ in problem 1, $\langle i \rangle_1$, can be expressed as $\langle i \rangle_1 = \delta U$, and net current across the plane $\theta = \pi/2$ in problem 2, $\langle i \rangle_2$, as $\langle i \rangle_2 = \beta E$. The condition of streaming potential implies that $\langle i \rangle = \langle i \rangle_1 + \langle i \rangle_2 = 0$, and, therefore, $E/U = -\delta/\beta$

(2)

四、結論與討論

Figure 2 shows the variation of (E^*/U^*) as a function of κa at various scaled surface potential ϕ_r . As can be seen from this figure, for a fixed ϕ_r , (E^*/U^*) approaches a constant value for both $\kappa a \rightarrow 0$ and $\kappa a \rightarrow \infty$. If ϕ_r is low, the variation of (E^*/U^*) has a minimum at a medium κa , as shown in Fig.2(a). On the other hand, if ϕ_r is sufficiently high, the minimum disappears, and a maximum may occur, as illustrated in Fig.2(b). The rationale behind these observations is elaborated below. According to its definition, $(E^*/U^*) = -\delta/\beta$, δ and β being the net currents across the plane $\theta = \pi/2$ in problems 1 and 2, respectively, suggests that $I_\theta(r^*)$ comprises two parts: the current due to the convective motion of liquid phase, I_{Ac} , and that due to the diffusion of ionic species, I_{Ad} . Define

$$\delta_c = \left(\int_1^{a/b} I_{\theta,c} dr^* \right)_{\text{problem 1}}, \quad \beta_c = \left(\int_1^{a/b} I_{\theta,c} dr^* \right)_{\text{problem 2}}$$

$$\delta_d = \left(\int_1^{a/b} I_{\theta,d} dr^* \right)_{\text{problem 1}}, \quad \beta_d = \left(\int_1^{a/b} I_{\theta,d} dr^* \right)_{\text{problem 2}}$$

$$\delta = \delta_c + \delta_d$$

$$\beta = \beta_c + \beta_d$$

For problem 1, the spatial variation of Ψ at two levels of κa is summarized in Table 1, and the corresponding variations in G_1 and G_2 are presented in Figs.3(a) and (3b) respectively. Table 1 suggests that circulation flow occurs. Also, $(\partial \Psi / \partial r^*)$ is insensitive to the variation in κa . On the other hand, both G_1 and G_2 are relatively sensitive to the variation in κa , as suggested by Figs.3(a) and 3(b). Note that in this problem, the boundary condition for Ψ at $r^* = 1$, Eq.(13e), is nonhomogeneous, and the boundary conditions for G_1 and G_2 at $r^* = a/b$, Eqs.(13b) and (13d), are homogenous. If $\kappa a \rightarrow 0$, the double layer is thick, and the variation in Ψ as r^* varies is insensitive. Also, as pointed previously, $(\partial \Psi / \partial r^*)$ is also insensitive to the variation in κa . According to Eqs.(20a) and (21a), suggests that δ_c is almost a constant. Furthermore, if $\kappa a \rightarrow 0$, implies that δ_d is negligible, and, therefore, δ is roughly constant. The fact that δ_c , δ_d , and δ all approach constant as $\kappa a \rightarrow 0$ are shown in Figs.4(a) and 4(b). As κa increases, the variation of ϕ_1 as r^* varies becomes steeper, and the contribution due to the term

$[\exp(\phi_r\phi^*_1)-\exp(\alpha\phi_r\phi^*_1)]$ in Eq.(20a) becomes less significant. According to Eq.(21a), δ_c decreases with κa , as can be seen from Figs.4(a) and 4(b). These figures also reveal that if κa is further increased, δ_c may change its sign and have a minimum. This is because that if κa is large, the contribution to δ_c by the term $[\exp(\phi_r\phi^*_1)-\exp(\alpha\phi_r\phi^*_1)]$ is significant for the interval $r^*\leq 1/\kappa a$ only. In this case a slight variation in $(\partial\Psi/\partial r^*)$ with κa becomes important. It can be inferred that $\delta_c\rightarrow 0$ as $\kappa a\rightarrow\infty$. Figures 4(a) and 4(b) also reveal that δ_d may have a maximum, as κa varies. This is because that the gradient of equilibrium concentration increases with κa , and, therefore, the effect of ionic diffusion is enhanced. However as κa increases, since $\nabla\phi_1$, or the electric field, also increases, it is harder for ion cloud around a particle to be polarized. The net effect is that δ_d exhibits a local maximum. The fact that δ has a minimum, and, therefore, (E^*/U^*) has a minimum, is due to these behaviors of δ_c and δ_d .

Figure 5(a) illustrates the spatial variation of ψ in problem 2 at two levels of κa , and the corresponding variations in G_1 and G_2 are presented in Figs 5(b) and (5c) respectively. Contrary to the results of problem 1, $(\partial\Psi/\partial r^*)$ is sensitive to the variation in κa in problem 2, but G_1 and G_2 become relatively insensitive to the variation in κa . In this problem, the boundary condition for ψ at $r^*=1$, Eq.(13e), is homogeneous, and the boundary conditions for G_1 and G_2 at $r^*=a/b$. Eqs.(13b) and (13d), are nonhomogenous. Figures 6(a) and 6(b) illustrate respectively the variations of β and β_c as a function of κa at two levels of ϕ_r . As can be seen from Fig.6(a), β approaches a constant as ϕ_r . This can be explained by employing the reasoning adopted in problem 1 for the variation of δ . This is why (E^*/U^*) in Fig.2 approaches a constant as $\kappa a\rightarrow 0$. Figure 6(a) reveals that $|\beta|$ decreases with the increase in κa . This is because that $\beta_c\ll\beta_d$, as can be judged from Figs.6(a) and 6(b), and $\beta\cong\beta_d$. Similar to the behavior of δ_d , $|\beta_d|$ decreases with the increase in κa . Figure 6(b) reveals that, if $\kappa a\rightarrow 0$, then $\beta_c\cong 0$. This is mainly due to the behavior of the spatial variation of ψ in problem 2, illustrated in Fig.5(a). Similar to the variation of δ_c , $|\beta_c|$ becomes more appreciable if κa becomes larger. However, a further increase in κa leads to a smaller, and as $\kappa a\rightarrow\infty$, $|\beta_c|\rightarrow 0$.

If ϕ_r is low, the minimum in the (E^*/U^*) against κa curve shown in Fig.2(a) is mainly due to the behavior of δ , which has a minimum as κa varies, as illustrated in Fig.4(a). However, as ϕ_r increases, the effect of β on (E^*/U^*) becomes more significant. According to Fig.6(a), $|\beta|$ decreases with κa , and therefore, the minimum in the (E^*/U^*) against κa curve is less appreciable, and may even vanish if ϕ_r is sufficiently high. Also, at a sufficiently high ϕ_r and large κa , the effect of the maximum of δ_d exceeds that of the minimum of δ_c . This leads to a maximum in the sum $\delta=\delta_c+\delta_d$, as shown in Fig.4(b), and, therefore, a maximum in (E^*/U^*) against κa curve as illustrated in Fig.2(b).

Figure 7 shows the variation of (E^*/U^*) as a function of ϕ_r at different κa . This figure reveals that for a fixed κa , (E^*/U^*) increases with the increase in ϕ_r , as expected. Also, for a fixed ϕ_r , (E^*/U^*) increases with the increase in κa . This is because that the larger the

κa , the thinner the double layer, and the greater the concentration gradient.

Figure 8 illustrates the variation of (E^*/U^*) as a function of κa at two different volume fractions of particle, measured by $H (= (a/b)^3)$. As suggested by this figure, the effect of the volume fraction of particle on the behavior of (E^*/U^*) is only quantitative, i.e., the qualitative behavior of (E^*/U^*) against κa curve at a high H is similar to that at a low H . A comparison between Figs.8(a) and 8(b) reveals that for a fixed ϕ_r , (E^*/U^*) increases with the volume fraction of particles.

ACKNOWLEDGMENT

This work is partially financially supported by the National Science Council of the Republic of China.

五、參考文獻

1. S.R. de Groot, P. Mazur, and J.Th.G. Overbeek, *J. Chem. Phys.* **20**, 1825 (1952)
2. H. Ohshima, T.W. Healy, L.R. White, and R.W. O'Brien, *J. Colloid Interface Sci.* **80**, 1299 (1984).
3. S. Levine and G.H. Neale, *J. Colloid Interface Sci.* **47**, 520 (1974).
4. S. Kuwabara, *J. Phys. Soc. Japan* **14**, 527 (1959).
5. S. Levine, G.H. Neale, and N. Epstein, *J. Colloid Interface Sci.* **57**, 421 (1976).
6. H. Ohshima, *J. Colloid Interface Sci.* **188**, 481 (1997).
7. M.W. Kozak and E.J. Davis, *J. Colloid Interface Sci.* **127**, 497 (1989).
8. M.W. Kozak and E.J. Davis, *J. Colloid Interface Sci.* **129**, 166 (1989).
9. E. Lee, J.W. Chu, and J.P. Hsu, *J.P. J. Colloid Interface Sci.* **205**, 65 (1998).
10. H. Ohshima, *J. Colloid Interface Sci.* **208**, 295 (1998).
11. E. Lee, J.W. Chu, and J.P. Hsu, *J. Colloid Interface Sci.* **209**, 240 (1999).
12. R.W. O'Brien and L.R. White, *J. Chem. Soc. Faraday Trans. 2* **74**, 1607 (1978).

六、圖表

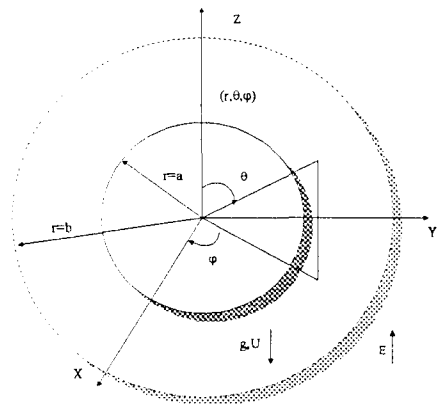
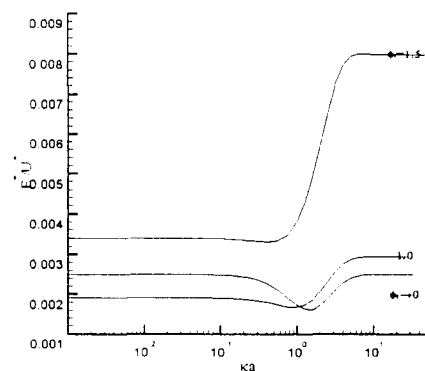


Fig.1. Schematic representation of cell model, where a particle of radius a is surrounded by a spherical liquid shell of radius b . The sedimentation of particles induces an electric field E in the z -dir



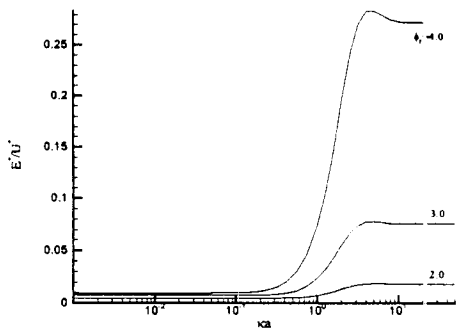


Fig2(b)

Fig.2. Variation of E^*/U^* as a function of Ka at various scaled surface potential ϕ_r for the case $H=0.5$. Key: $\alpha=1, Pe_1=Pe_2=0.01$.

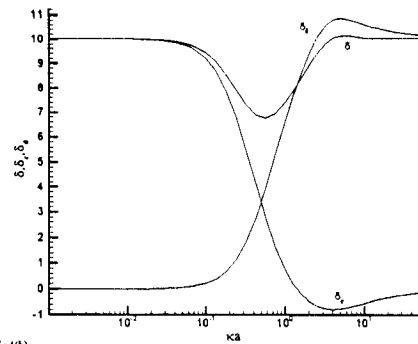


Fig4(b)

Fig.4. Variation of δ_c, δ_d and δ as a function of Ka for the case $H=0.5, \phi_r=1$, (a), and $\phi_r=3$, (b). Key: same as Fig.2.

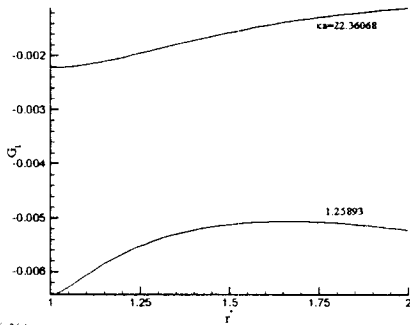


Fig3(a)

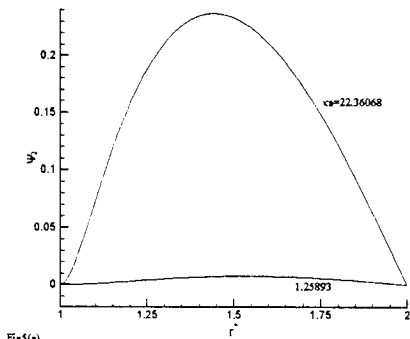


Fig5(a)

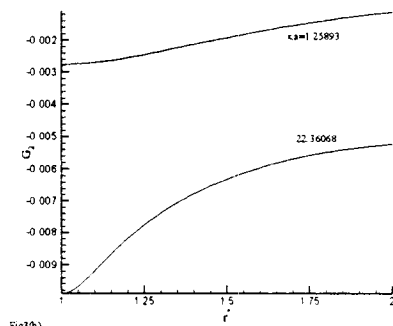


Fig3(b)

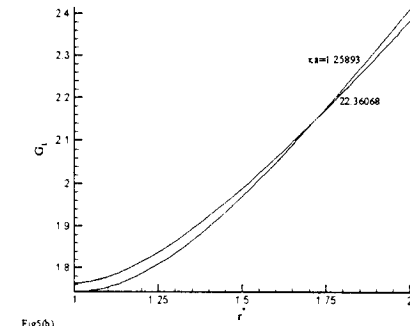


Fig5(b)

Fig.3. Variations of G_1 , (a), and G_2 , (b), as a function of r^* at different values of Ka in problem 1 for the case $H=0.5$ and $\phi_r=1$. Key: same as Fig.2.

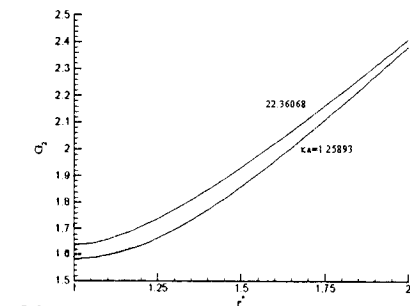


Fig5(c)

Fig.5. Variation of Ψ_2 as a function of r^* , (a), that of G_1 , (b), and that of G_2 , (c), at different values of Ka in problem 2 for the case $H=0.5$ and $\phi_r=1$. Key: same as Fig.2.

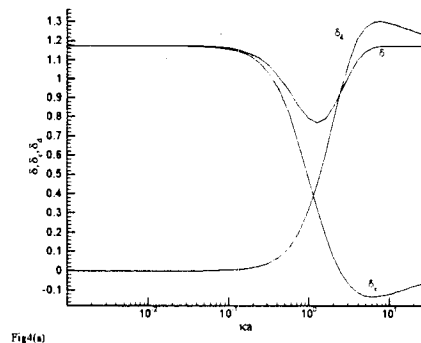
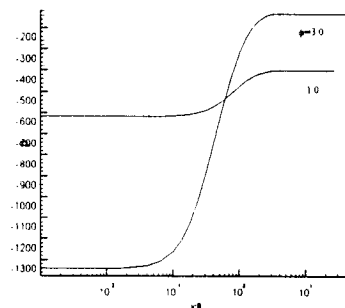


Fig4(a)



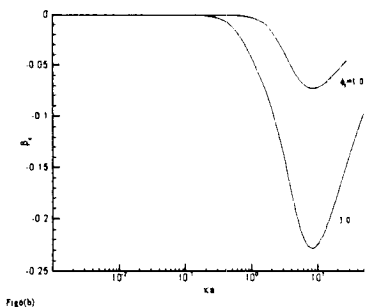


Fig. 6. Variation of β as a function of κa , (a), and that of β_C , (b), for the case $H=0.5$ and $\Phi_r=1$. Key: same as Fig.2.

1.20215	0.012001E+00	0.011280E+00	1.17810E-03
1.30866	0.009263E+00	0.008298E+00	1.58388E-03
1.40245	0.578371E+00	0.577317E+00	1.82236E-03
1.50000	0.522292E+00	0.521249E+00	1.99687E-03
1.59755	0.445829E+00	0.444883E+00	2.12189E-03
1.71378	0.333601E+00	0.332860E+00	2.22122E-03
1.79785	0.241642E+00	0.241094E+00	2.26782E-03
1.90160	0.119864E+00	0.119588E+00	2.30261E-03
1.95199	0.587403E-01	0.586045E-01	2.31187E-03
1.99039	0.117715E-01	0.117443E-01	2.31067E-03
1.99940	0.737979E-03	0.736272E-03	2.31307E-03

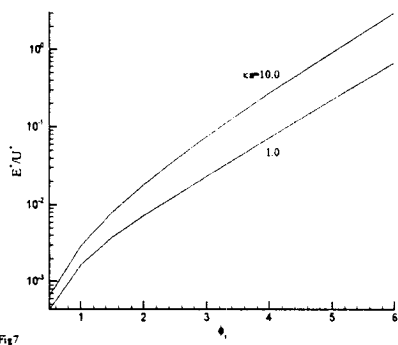


Fig. 7. Variation of E^*/U^* as a function of Φ_r at two different κa for the case $H=0.5$ and $\Phi_r=1$. Key: same as Fig.2.

Table 1. Variation of Ψ_1 as a function of r^* at different values of κa for the case $H=0.5$, $\alpha=1$, and $\phi_r=1$. D denotes the percent difference in Ψ_1 defined by $100\% \alpha | \psi_1(\kappa a = 1.25893) - \psi_1(\kappa a = 22.36068) | / \psi_1(\kappa a = 1.25893)$.

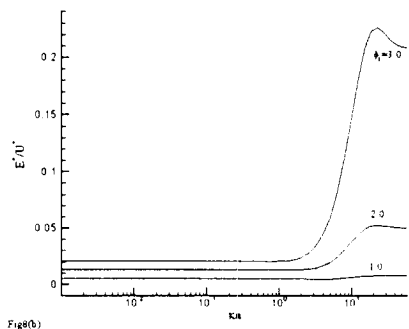
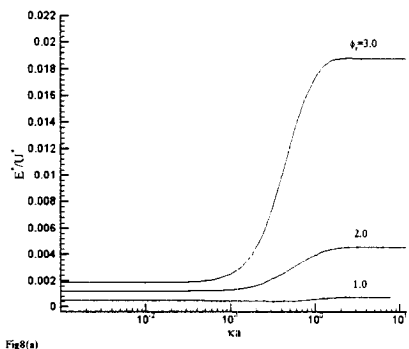


Fig. 8. Variation of E^*/U^* as a function of κa at various Φ_r . (a) $H=0.25$, (b) $H=0.833$. Key: same as Fig. 2.

r^*	Ψ_1		D (%)
	$\kappa a=259$	$\kappa a=22.36$	
1.00541	0.505340E+00	0.505338E+00	3.95773E-06
1.04801	0.542492E+00	0.542376E+00	2.13828E-06
1.09840	0.575858E+00	0.575528E+00	5.73058E-04